Title	Ultraviolet stimulated emission in AlGaN layers grown on sapphire substrates using ammonia and plasma-assisted molecular beam epitaxy
Authors	Rzheutski, Mikalai V.;Lutsenko, Evgenii V.;Vainilovich, Aliaksei G.;Svitsiankou, Illia E.;Nahorny, Aliaksei V.;Yablonskii, Gennadii P.;Zubialevich, Vitaly Z.;Petrov, Stanislav I.;Alexeev, Alexey N.;Nechaev, Dmitrii V.;Jmerik, Valentin N.
Publication date	2020-03-03
Original Citation	Rzheutski, M. V., Lutsenko, E. V., Vainilovich, A. G., Svitsiankou, I. E., Nahorny, A. V., Yablonskii, G. P., Zubialevich, V. Z., Petrov, S. I., Alexeev, A. N., Nechaev, D. V. and Jmerik, V. N. 'Ultraviolet Stimulated Emission in AlGaN Layers Grown on Sapphire Substrates using Ammonia and Plasma-Assisted Molecular Beam Epitaxy', Physica Status Solidi (A), doi: 10.1002/pssa.201900927
Type of publication	Article (peer-reviewed)
Link to publisher's version	https://onlinelibrary.wiley.com/doi/abs/10.1002/pssa.201900927 - 10.1002/pssa.201900927
Rights	© 2020. This article is protected by copyright. All rights reserved. This is the peer reviewed version of the following article: Rzheutski, M.V., Lutsenko, E.V., Vainilovich, A.G., Svitsiankou, I.E., Nahorny, A.V., Yablonskii, G.P., Zubialevich, V.Z., Petrov, S.I., Alexeev, A.N., Nechaev, D.V. and Jmerik, V.N. (2020), Ultraviolet Stimulated Emission in AlGaN Layers Grown on Sapphire Substrates using Ammonia and Plasma#Assisted Molecular Beam Epitaxy. Phys. Status Solidi A. Accepted Author Manuscript, which will be published in final form at https://doi.org/10.1002/pssa.201900927. This article may be used for non-commercial purposes in accordance with Wiley Terms and Conditions for Self-Archiving
Download date	2024-04-23 12:02:54
Item downloaded from	https://hdl.handle.net/10468/9745

University College Cork, Ireland
Coláiste na hOllscoile Corcaigh

Ultraviolet stimulated emission in AlGaN layers grown on sapphire substrates using ammonia and plasma-assisted molecular beam epitaxy

Mikalai V. Rzheutski, Evgenii V. Lutsenko, Aliaksei G. Vainilovich, Illia E. Svitsiankou, Aliaksei V. Nahorny, Gennadii P. Yablonskii, Vitaly Z. Zubialevich, Stanislav I. Petrov, Alexey N. Alexeev, Dmitrii V. Nechaev, Valentin N. Jmerik*

Dr. Mikalai V. Rzheutski, Dr. Evgenii V. Lutsenko, Mr. Aliaksei G. Vainilovich, Mr. Illia E. Svitsiankou, Mr. Aliaksei V. Nahorny, Prof. Gennadii P. Yablonskii
Institute of Physics of NAS of Belarus, 68 Nezalezhnasci Ave, Minsk, 220072, Belarus
E-mail: m.rzheutski@ifanbel.bas-net.by

Dr. Vitaly Z. Zubialevich
Tyndall National Institute, University College Cork, Lee Maltings, Dyke Parade, Cork, T12R5CP, Ireland

Dr. Stanislav I. Petrov, Dr. Alexey N. Alexeev
SemiTEq JSC, 27 Engels Ave, Saint-Petersburg, 194156, Russia

Mr. Dmitrii V. Nechaev, Dr. Valentin N. Jmerik
Ioffe Institute, 26 Polytekhnicheskaya, Saint-Petersburg, 194021, Russia

Keywords: AlGaN, AlN, molecular beam epitaxy, structural properties, stimulated emission

Ammonia and plasma-assisted (PA) molecular beam epitaxy modes are used to grow AlN and AlGaN epitaxial layers on sapphire substrates. It is determined that the increase of thickness of AlN buffer layer grown by ammonia-MBE from 0.32 μm to 1.25 μm results in the narrowing of 101 X-Ray rocking curves whereas no clear effect on 002 X-Ray rocking curve width is observed. It is shown that strong GaN decomposition during growth by ammonia-MBE causes AlGaN surface roughening and compositional inhomogeneity, which leads to deterioration of its lasing properties. AlGaN layers grown by ammonia-MBE at optimized temperature demonstrate stimulated emission (SE) peaked at $\lambda = 330$ nm, 323 nm, 303 nm and 297 nm with the SE threshold values of 0.7 MW cm^{-2}, 1.1 MW cm^{-2}, 1.4 MW cm^{-2} and 1.4 MW cm^{-2}, respectively. In comparison to these, AlGaN layer grown using PA-MBE pulsed modes (migration-enhanced epitaxy, metal-modulated

This article has been accepted for publication and undergone full peer review but has not been through the copyediting, typesetting, pagination and proofreading process, which may lead to differences between this version and the Version of Record. Please cite this article as doi: 10.1002/pssa.201900927.

epitaxy, and droplet elimination by thermal annealing) shows a SE with a relatively low threshold (0.8 MW cm^{-2}) at the considerably shorter wavelength of λ = 267 nm.

1. Introduction

To date GaN, AlN, and their ternary alloys are considered the basic materials for optoelectronic semiconductor devices operating in the A-, B-, and C-ultraviolet (UV) spectral regions. The compact and efficient UV semiconductor devices are highly requested for a variety of important applications, including solar- and visible-blind photodetectors, air/water disinfection systems, spectral analysis, polymerization, secure communication, etc.[1] III-nitrides (III-N) have also attracted great attention as materials for high power and RF electronics, which is caused by numerous of their outstanding properties such as a wide bandgap, high electric breakdown field, and high electron saturation velocity.[2] However, wide implementation of III-N-based heterostructures, face some technical problems limiting their efficiency and commercial availability.

The main difficulty is a high cost of bulk GaN or AlN crystals, resulting in usage of foreign substrates for heteroepitaxy (SiC, sapphire, Si) and leading to a high density of structural defects. Furthermore, expanding the spectral range of AlGaN-based optoelectronics to a deeper UV requires an increase in AlN fraction of AlGaN alloy which results in degradation of AlGaN structural quality because of the high Al–N bond strength and, therefore, lower Al adatom mobility.[3] Besides the known difficulty in *p*-doping of III-Ns, due to a significant increase of donor activation energy as the Al fraction increases, *n*-doping of high Al content AlGaN becomes challenging too.[4] Last but not least, much lower light extraction efficiencies from *c*-plane AlGaN-based emitters with high AlN mole fractions are expected. This is caused by the change of the order in the valence sub-bands between GaN and AlN in such a way that the probability of light emitted along the *c*-axis significantly reduces in AlGaN with high Al content.[5]

In most cases, the UV-optoelectronics devices were fabricated using metalorganic chemical vapor deposition (MOCVD). This technology in particular, demonstrated a significant progress from initial optically pumped UV lasers to recent implementation of the first sub-300 nm UV laser diode on the bulk AlN substrate.[6-10] Nevertheless, molecular beam epitaxy (MBE) also demonstrated optically pumped UV-lasing from AlGaN quantum well structures grown on *c*-sapphire substrates, with a threshold power density comparable to that obtained using MOCVD.[11,12] MBE which is less suitable for mass production, has some potential advantages, such as lower incorporation levels of impurities and a wider range of in-situ monitoring tools. In addition, this technology allows for the formation of quantum-sized heterostructures with monolayer-range sharpness at the interfaces. Moreover, typically lower growth temperatures applied in MBE inhibit the undesired diffusion of dopant atoms from conductive layers to the active region of laser diode heterostructures.[13]

In this work, we report on the optimization of MBE of AlN buffer layers and investigate the influence of MBE growth conditions on alloy homogeneity and optical properties of AlGaN layers.

2. Experimental methods

All the growth experiments were performed in an STE3N2 (SemiTEq) MBE reactor on 2-inch single side polished sapphire (0001) substrates with a surface misorientation of 0.2° by using both ammonia (NH_3) and plasma-assisted (PA) modes. The pre-growth substrate preparation included annealing and nitridation steps as has been described in our earlier work. [14] The structures were studied by scanning electron microscope (SEM, Carl Zeiss Supra 40), atomic force microscope (AFM, Nanoflex Solar LS) and X-ray diffraction (PANalytical X'pert PRO) analysis. Room-temperature (RT) photoluminescence (PL) and stimulated emission (SE) of AlGaN layers were excited with the 5th harmonic of emission of a Nd:YAG laser (λ_{exc} = 213 nm) and detected with a MayaPro spectrometer (Ocean Optics). As grown 2-inch wafers were cleaved into two halves with

single flat facets to provide a single-pass geometry for the SE measurements. The excitation emission was focused into a strip (~2 mm length), oriented normally to the cleaved edge, and the output emission was collected from the cleaved edge. The single-pass geometry minimized the influence of facet quality on the measured SE threshold value. The polarized SE was measured using a Rochon prism located between the sample edge and the light collecting lens. To determine an absorption edge, the RT transmittance spectra were measured using a deuterium lamp.

3. Results and discussion

3.1. NH_3-MBE grown AlN buffers and AlGaN layers

3.1.1. AlN buffer layer

In our recent work we considered the effect of growth temperature and ammonia flow on surface morphology and structural properties of 0.32-μm -thick AlN epilayers.[14] Here we extend our study on the effect of AlN thickness. The epitaxy for all the NH_3-MBE grown AlN layers was initiated with a step of a relatively low growth rate of ~0.05 μm h^{-1} (first 70 nm) followed by a gradual increase to its normal rate of 0.2 μm h^{-1}. Two series of AlN buffer layers of different thickness (0.32 μm and 1.25 μm) were grown at varied growth temperature s T_g (from 800 °C to 1190 °C) and NH_3 flow (from 30 sccm (standard cubic centimeters per minute) to 100 sccm). Other growth details can be found elsewhere. [14]

In **Figure 1**, SEM images of the 1.25-μm -thick AlN layers grown at various conditions can be seen. As seen from the SEM images, a low growth temperature of 1010 °C leads to the formation of misoriented crystallites. Ammonia flow rate of 100 sccm and growth temperature of 1085 °C resulted in the formation of flat terraces having a width of up to ~1 μm without hillocks, misoriented crystals and polycrystals observed in other layers. The same terrace-like morphology was also observed by AFM for the AlN layer grown at a higher ammonia flow rate of 200 sccm (not shown). The higher growth temperature leads to a formation of prismatic hills. A very similar behavior was observed for the series of thin AlN layers.[14]

The full widths at half maximum (FWHM) of X-ray rocking curves (XRC) for 101 and 002 XRD reflections are shown in **Figures 2** as a function of temperature. Both the series of AlN layers demonstrate a tendency of XRC peaks narrowing with growth temperature increase (except for two 0.32-μm -thick AlN layers grown at the highest studied temperature of 1190°C) which means the reduction of all threading dislocation density (TDD) with both screw and edge components.[15] This behavior can be explained by an enhanced mobility of Al adatoms at elevated growth temperatures.[16, 17] The lowest TDD values of $n_{edge} \sim 5.9\times10^{9}$ cm^{-2} and $n_{screw} \sim 2.2 \times 10^{7}$ cm^{-2} were estimated for the 1.25-μm -thick AlN layer deposited at the NH_3 flow rate of 50 sccm and T_g=1190 °C.[15] . It should be noted that a reduction in the FWHM values with the buffer layer thickness was observed for the asymmetric XRC peak 101 (**Figure 2, *a***) only, while the widths of the symmetric peak 002 did not reveal a significant difference for the series of layers with the different thickness (**Figure 2, *b***). This contradicts results reported by other authors, who demonstrated a reduction of both edge and screw TDD with an increase in AlN thickness.[18, 19]

The root mean square (RMS) surface roughness values for the AlN layers measured at a scan area of 5 × 5 μm^2 are plotted in **Figure 3** as a function of growth temperature. As seen from the figure, no clear dependence of RMS roughness on growth conditions can be observed. One can just notice a somewhat rougher surface for the thicker AlN layers. As expected from **Figure 1**, the lowest roughness (≈ 0.7 nm) was measured for the AlN layer grown at a temperature of 1085°C and NH_3 flow of 100 sccm, demonstrating a terrace-like surface morphology (the estimated TDD values for the layer were of $n_{edge} \sim 8.9 \times 10^{10}$ cm^{-2} and $n_{screw} \sim 3.5 \times 10^{8}$ cm^{-2}).

3.1.2. AlGaN layers

For the growth of AlGaN layers, a temperature of 1085 °C and NH_3 flow of 100 sccm were taken as optimal conditions providing a reasonable compromise between the surface roughness and the structural quality of AlN/sapphire templates. AlGaN layers were grown using buffer structures consisting of 0.32 μm thick AlN followed by 0.14 μm thick gradient-composition $Al_yGa_{1-y}N$. The

composition y in the layer was varied from 1 to x by a linear decrease of Al flow (Ga and NH_3 flows were kept constant), where x is the AlN mole fraction of the upper $Al_xGa_{1-x}N$ layer, which had the fixed thickness of 0.15 μm in all the experiments. The aluminum composition x in the upper layer was varied within the series, depending on growth conditions. The relatively small AlN buffer thickness of 0.32 μm was chosen to provide a smoother initial surface for AlGaN growth. In total, two series of AlGaN layers were grown by ammonia MBE. The first series was prepared to investigate the effect of growth temperature on AlGaN surface roughness and its optical properties, and the optimal temperature from this experiment was then used for the second series where the Ga/Al ratio was varied.

All the AlGaN layers within the first series were grown at a nominally fixed Al/(Ga+Al) flux ratio of ≈ 0.3 and NH_3 flow of 100 sccm. The growth temperature of the gradient-composition and final top AlGaN layers was varied from 860°C to 950°C.

First, the AlGaN surface morphology was assessed by AFM. The corresponding AlGaN RMS surface roughness is plotted as a function of growth temperature in **Figure 4** (circles), and can be seen to increases with temperature. An increased rate of GaN decomposition during the growth at elevated temperatures may be one of the possible explanations to this observation. It is known from the literature, that GaN surface morphology and growth rate are very sensitive to growth temperature due to the activation of GaN thermal decomposition. [20, 21] To provide further evidence, we carried out an additional experiment on GaN growth using exactly the same conditions as for our AlGaN. The GaN growth rate is also shown as a function of growth temperature **in Figure 4** (squares). Progressing thermal decomposition at temperatures above ≈ 870°C at the NH_3 flow of 100 sccm manifests itself through the noticeable decrease in the GaN growth rate.

Smoother AlGaN surfaces were achieved at growth temperatures ranging from 870°C to 920°C, which correspond to only a moderate GaN thermal decomposition, i.e., resulting in growth rate reduction of lower than about 5-6%. Temperatures outside of the range result in somewhat rougher

AlGaN surface morphologies. While the effect of the elevated temperatures can be explained by severe thermal decomposition of GaN fraction, the lower than optimal temperatures are assumed to degrade the surface morphology due to progressively decreasing adatom mobility.

The effect of the growth temperature on the localization degree of photogenerated carriers in AlGaN layers, was evaluated from measurements of the Stokes shift determined as energetic difference between PL band position and optical absorption edge.[22] As seen from **Figure 5** (circles), lower Stokes shifts are observed for the AlGaN layers grown at the temperatures again within the range of 870°C – 920°C, while a rise in the growth temperature above 940°C leads to a substantial rise of the Stokes shift. Generally, the similar temperature behaviors of the Stokes shift and RMS roughness are quite noticeable, which allows us to correlate the rougher surface morphology with the pronounced compositional inhomogeneity in our AlGaN, which was prepared outside the optimal range of growth temperatures.

The AlGaN layers grown at 860°C, 875°C and 905°C demonstrated stimulated emission near $\lambda = 300$ nm, with threshold values of 2 MW cm^{-2}, 1.4 MW cm^{-2} and 9 MW cm^{-2} respectively (**Figure 5**, squares). It should be noted that the lowest SE threshold corresponds to the sample with the lowest RMS roughness of ≈ 1.3 nm. An increase of AlGaN growth temperature above ~880°C leads to a drastic deterioration of lasing properties which is likely caused by the negative influence of both the surface roughening and the AlGaN alloy disordering.

The second series of AlGaN layers was grown by NH_3-MBE at the optimized temperature of 870°C with varied Al/(Ga+Al) ratios resulting in the following AlN mole fractions in AlGaN alloys: 0.24, 0.31, 0.38 and 0.43, as estimated from the corresponding transmittance spectra measurements. The layers demonstrated SE at $\lambda = 330$ nm, 323 nm, 303 nm and 297 nm with the SE thresholds of 0.7 MW cm^{-2}, 1.1 MW cm^{-2}, 1.4 MW cm^{-2} and 1.4 MW cm^{-2}, respectively. The SE of all the layers was found to be transverse-electric (TE) polarized with spectral linewidths of 2.1-2.8 nm, whereas the corresponding spontaneous recombination PL spectra were 10-14 nm broad. An example of SE

spectra for the $Al_{0.24}Ga_{0.76}N$ layer is shown in **Figure 6**. The Stokes shift values for the samples of the second series was found to be lower than 20 meV which indicates a good alloy homogeneity of AlGaN in these layers.

3.2. PA-MBE grown AlGaN layer

Recently, we have demonstrated a possibility of PA-MBE growth of an AlN buffer layer with a relatively small surface roughness of 0.9 nm by using an approach developed earlier.[14,23,24] In this work, we used the same approach to prepare the AlN buffer for subsequent AlGaN growth. The AlN buffer layer was grown at temperature of 805°C and consisted of 80 nm thick migration-enhanced epitaxy (MEE) nucleation sublayer, 0.4 μm -thick metal-modulated epitaxy (MME) sublayer and 0.33 μm thick sublayer grown at continuous PA-MBE metal-rich conditions. The nitrogen flow and plasma power were 3 sccm and 200 W, respectively. A 0.15 μm thick $Al_{0.7}Ga_{0.3}N$ layer was grown at the temperature of 740°C using the droplet elimination by thermal annealing (DETA) mode.[24] In this mode, AlGaN growth is performed by the cyclic switching between two stages: each 2 min long phase of continuous AlGaN growth in Ga-rich conditions was followed by a 0.5 min long annealing step with all the precursors (including nitrogen plasma) switched off. The annealing phase was introduced to evaporate the excess of Ga adatoms accumulated during the growth phase and prevent the undesirable formation of Ga droplets. The Ga and N* flows, and the phase durations were tuned accurately to provide a full suppression of Ga droplet formation.

The surface of the PA-MBE-grown $Al_{0.7}Ga_{0.3}N$ layer was found to be not particularly smooth; a corresponding RMS surface roughness of ~3 nm was estimated from the $5 \times 5\ \mu m^2$ AFM map shown in **Figure 7**. Despite this, the layer demonstrated a TE-polarized SE peaked at $\lambda = 267$ nm with a relatively low threshold of 0.8 MW cm^{-2} (**Figure 8**). The spectral linewidth of the emission decreased from ~16 nm to ~6 nm as SE occurred. It is worth noting that the threshold value is even lower than that of the shortest wavelength AlGaN layer grown by ammonia-MBE. Such an

improvement is most likely caused by the thicker AlN buffer layer resulting in an improved structural quality (TDD values of $n_{edge} \sim 3.4 \times 10^{10}$ cm^{-2} and $n_{screw} \sim 3.3 \times 10^{9}$ cm^{-2} in a similar AlN buffer layer were estimated in our recent work).[14]

Taking into account the relatively low threshold value (despite the relatively rough surface morphology), one could expect a substantial improvement of AlGaN lasing properties after a proper optimization of PA-MBE growth conditions.

4. Conclusions

In this work, we investigated different MBE approaches to grow AlN and AlGaN epitaxial layers on sapphire substrates. Ammonia MBE growth conditions of AlN buffer were optimized to achieve RMS roughness below 1 nm. It was shown that the increase of AlN layer thickness from 0.32 μm to 1.25 μm results in the decrease of 101 X-Ray rocking curve FWHM whereas no effect was observed on 002 X-Ray rocking curve FWHM. The lowest estimated dislocation density values for the 1.25 μm -thick AlN layer were $n_{edge} \sim 5.9 \times 10^{9}$ cm^{-2} and $n_{screw} \sim 2.2 \times 10^{7}$ cm^{-2}. Upon optimization of AlGaN growth temperature, the series of 0.15-μm -thick layers with varied Ga/Al flux ratios was grown by ammonia MBE. All these AlGaN layers demonstrated SE peaked at $\lambda = 330$ nm, 323 nm, 303 nm and 297 nm with the SE threshold values of 0.7 MW cm^{-2}, 1.1 MW cm^{-2}, 1.4 MW cm^{-2} and 1.4 MW cm^{-2}, respectively. Pulsed PA-MBE modes (MEE, MME, DETA) were used to grow a 0.15-μm -thick $Al_{0.7}Ga_{0.3}N$ layer. Despite the rather rough surface (RMS roughness of ≈ 3 nm), the layer exhibited SE at $\lambda = 267$ nm with a relatively low threshold value of 0.8 MW cm^{-2}. The obtained results demonstrate the possibility of growth of laser quality AlGaN-based heterostructures for UV applications by both ammonia and PA-MBE.

Acknowledgements
This work was supported in part by State programs of scientific research of Belarus "Photonics, opto- and micro-electronics"2.1.01, 2.1.04 and Russian Science Foundation Grant #19-72-30040.

Received: ((will be filled in by the editorial staff))
Revised: ((will be filled in by the editorial staff))
Published online: ((will be filled in by the editorial staff))

References

[1] Y. Nagasawa, A. Hirano, *Appl. Sci.* **2018**, *8*, 1264.

[2] U. K. Mishra, P. Parikh, Y. F. Wu, *Proc. IEEE* **2002,** *90*, 1022.

[3] S. Keller, S.P. DenBaars, *J. Cryst. Growth* **2003**, *248*, 479.

[4] P. Pampili, P.J. Parbrook, *Mater. Sci. Semicond. Process.* **2017**, *62*, 180.

[5] K.B. Nam, J. Li, M.L. Nakarmi, J.Y. Lin, H.X. Jiang, *Appl. Phys. Lett.* **2004**, *84*, 5264.

[6] X.-H. Li, T. Detchprohm, T.-T. Kao, M.M. Satter, S.-C. Shen, P. Douglas Yoder, R.D. Dupuis, S. Wang, Y.O. Wei, H. Xie, A.M. Fischer, F.A. Ponce, T. Wernicke, C. Reich, M. Martens, M. Kneissl, *Appl. Phys. Lett.* **2014,** *105*, 141106.

[7] T. Wunderer, C.L. Chua, Z. Yang, J.E. Northrup, N.M. Johnson, G.A. Garrett, H. Shen, and M. Wraback, *Appl. Phys. Express* **2011,** *4*, 092101.

[8] X.-H. Li, T. Detchprohm, T.-T. Kao, M.M. Satter, S.-C. Shen, P. Douglas Yoder, R.D. Dupuis, S. Wang, Y.O. Wei, H. Xie, A.M. Fischer, F.A. Ponce, T. Wernicke, C. Reich, M. Martens, M. Kneissl, *Appl. Phys. Lett.* **2014,** *105*, 141106.

[9] Q. Guo, R. Kirste, S. Mita, J. Tweedie, P. Reddy, B. Moody, Y. Guan, S. Washiyama, A. Klump, Z. Sitar, R. Collazo, *J. Appl. Phys.* **2019,** *126*, 223101.

[10] Z. Zhang, M. Kushimoto, T. Sakai, N. Sugiyama, L. J. Schowalter, C. Sasaoka, H. Amano *Appl. Phys. Express* **2019,** *12*, 124003.

[11] V.N. Jmerik,_ A.M. Mizerov, A.A. Sitnikova, P.S. Kop'ev, S.V. Ivanov, E.V. Lutsenko, N.P. Tarasuk, N.V. Rzheutskii, and G.P. Yablonskii, *Appl. Phys. Lett.* **2010**, *96*, 141112.

[12] S.V. Ivanov, S.V. Ivanov, D.V. Nechaev, A.A. Sitnikova, V.V. Ratnikov, M.A. Yagovkina, N.V. Rzheutskii, E.V. Lutsenko and V.N. Jmerik, *Semicond. Sci. Technol.* **2014**, *29*, 084008.

[13] S. Kotzea, W. Witte, B.-J. Godejohann, M. Marx, M. Heuken, H. Kalisch, R. Aidam, A. Vescan, *Electronics* **2019,** *8*, 377.

[14] A. Alyamani, E. V. Lutsenko, M. V. Rzheutski, V. Z. Zubialevich, A. G. Vainilovich, I. E. Svitsiankou, V. A. Shulenkova, G. P. Yablonskii, S. I. Petrov, A. N. Alexeev, *Jpn. J. Appl. Phys.* **2019**, *58*, SC1010.

[15] J. Xiong, J. Tang, T. Liang, Y. Wang, C. Xue, W. Shi, W. Zhang, *Appl. Surf. Sci.* **2010**, *257*, 1161.

[16] A. N. Alexeev, D. M. Krasovitsky, S. I. Petrov, V. P. Chaly, V. V. Mamaev, V. G. Sidorov, *Semiconductors* **2015**, *49*, 92.

[17] D. A. Neumayer, J. G. Ekerdt, *Chem. Mater.* **1996**, *8*, 9.

[18] W. Y. Fu, M. J. Kappers, Y. Zhang, C. J. Humphreys, M. A. Moram, *Appl. Phys. Express* **2011**, *4*, 065503.

[19] X.-H. Li, S. Wang, H. Xie, Y. O. Wei, T.-T. Kao, Md. M. Satter, S.-C. Shen, P. D. Yoder, T. Detchprohm, R. D. Dupuis, A. M. Fischer, F. A. Ponce, *Phys. Status Solidi B* **2015**, *252*, 1089.

[20] J. B. Webb, H. Tang, J. A. Bardwell, S. Moisa, C. Peters, T. MacElwee, *J. Cryst. Growth* **2001**, *230*, 584.

[21] A.N. Alexeev, B.A. Borisov, V.P. Chaly, D.M. Demidov, A.L. Dudin, D.M. Krasovitsky, Yu.V. Pogorelsky, A.P. Shkurko, I.A. Sokolov, M.V. Stepanov, A.L. Ter-Martirosyan, *MRS Internet J. Nitride Semicond. Res.* **1999**, *4*, e6.

[22] A. N. Pikhtin, H. H. Hegazy, *Semiconductors* **2009**, *43*, 1259.

[23] D. V. Nechaev, P. A. Aseev, V. N. Jmerik, P. N. Brunkov, Y. V. Kuznetsova, A. A. Sitnikova, V. V. Ratnikov, and S. V. Ivanov, *J. Cryst. Growth* **2013**, *378*, 319.

[24] D. V. Nechaev, P. N. Brunkov, S. I. Troshkov, V. N. Jmerik, S. V. Ivanov, *J. Cryst. Growth* **2015**, *425*, 9.

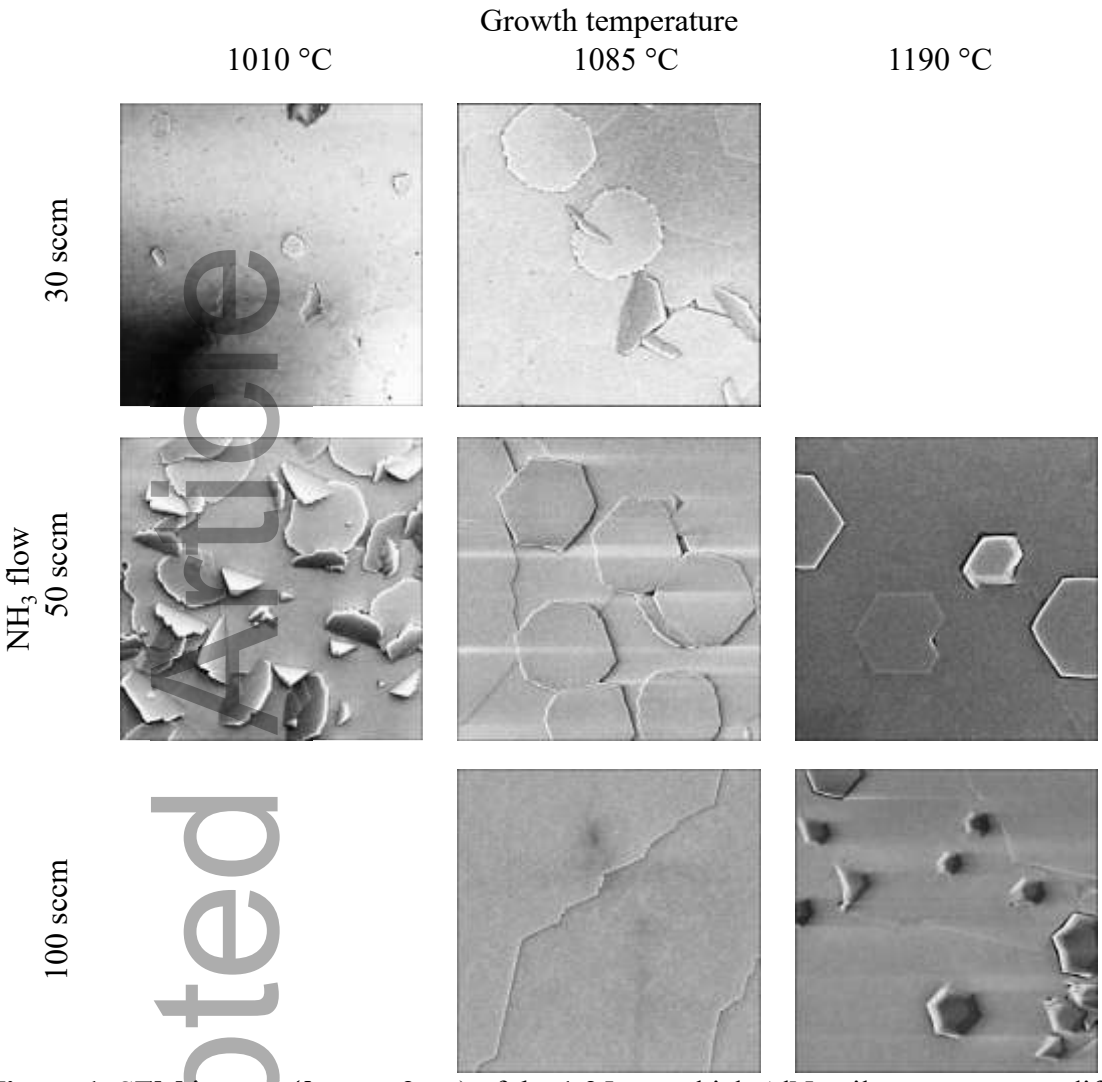

Figure 1. SEM images (2 μm × 2 μm) of the 1.25 -μm -thick AlN epilayers grown at different NH_3-MBE conditions.

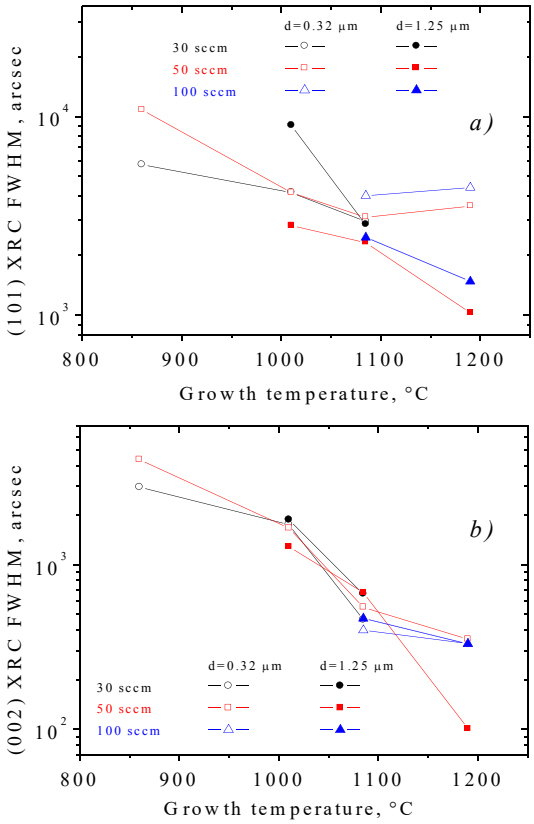

Figure 2. 101 (*a*) and 002 (*b*) XRC FWHM values of AlN layers grown by NH_3-MBE at different conditions.

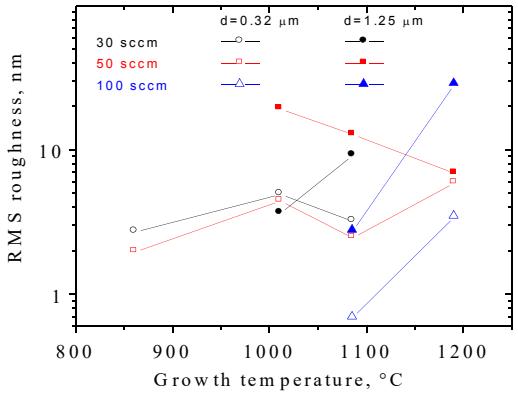

Figure 3. RMS surface roughness of AlN layers grown by NH_3-MBE at different conditions (5 μm × 5 μm AFM scans).

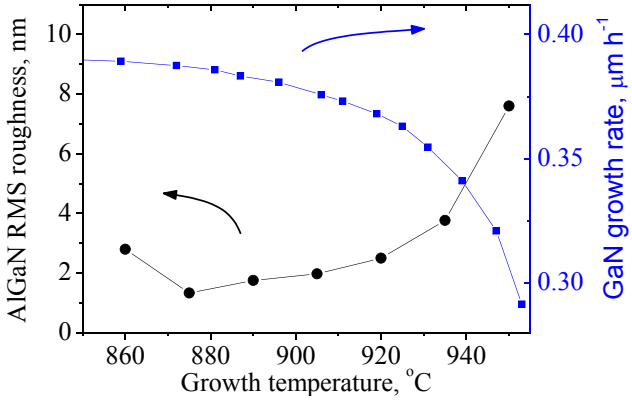

Figure 4. RMS surface roughness of AlGaN layers (5 μm × 5 μm AFM scans) and GaN growth rate as a function of growth temperature.

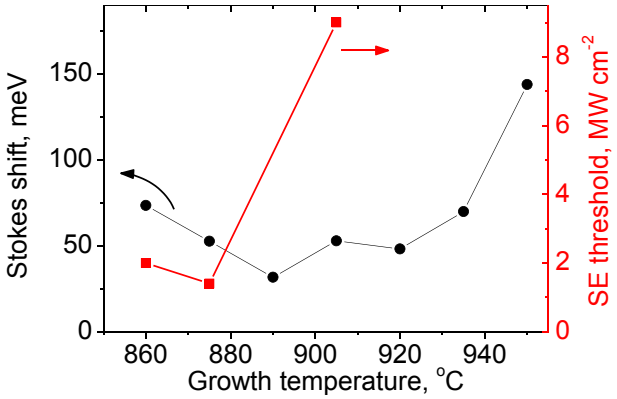

Figure 5. Stokes shift and SE threshold values of AlGaN layers as a function of growth temperature.

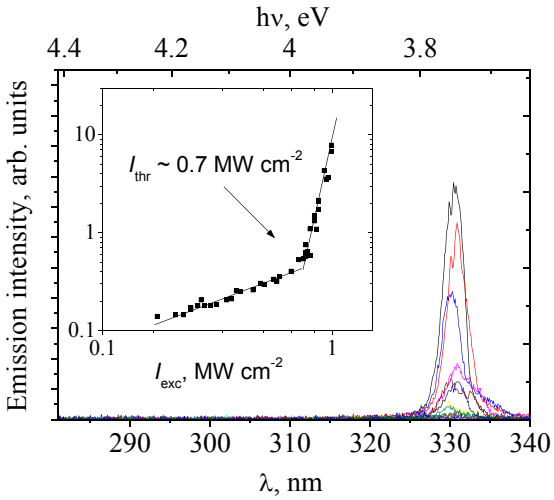

Figure 6. SE spectra for the NH_3-MBE grown $Al_{0.24}Ga_{0.76}N$ layer measured at different excitation levels. Inset shows the dependence of integrated emission on excitation level.

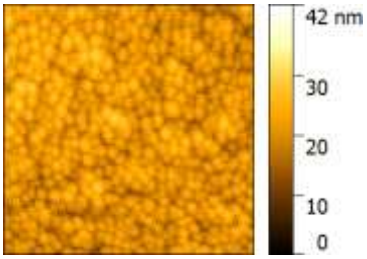

Figure 7. AFM scan (5 μm × 5 μm) of PA-MBE-grown $Al_{0.7}Ga_{0.3}N$ layer.

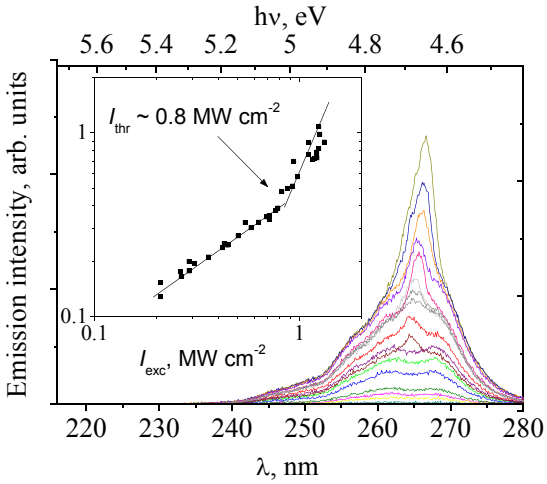

Figure 8. SE spectra for the PA MBE grown $Al_{0.7}Ga_{0.3}N$ layer measured at different excitation levels. Inset shows the dependence of integrated emission on excitation level.

Ammonia (NH_3) and plasma-assisted (PA) molecular beam epitaxy is used to grow AlN and AlGaN epitaxial layers on sapphire substrates. The effect of the growth conditions on the structural properties of AlN buffer as well as photoluminescence and stimulated emission of AlGaN layers grown by NH_3-MBE is shown. A stimulated emission in NH_3- and PA-MBE grown AlGaN layers with a relatively low threshold is demonstrated.

Keyword AlGaN, AlN, molecular beam epitaxy, structural properties, stimulated emission

Mikalai V. Rzheutski*, Evgenii V. Lutsenko, Aliaksei G. Vainilovich, Illia E. Svitsiankou, Aliaksei V. Nahorny, Gennadii P. Yablonskii, Vitaly Z. Zubialevich, Stanislav I. Petrov, Alexey N. Alexeev, Dmitrii V. Nechaev, Valentin N. Jmerik

Ultraviolet stimulated emission in AlGaN layers grown on sapphire substrates using ammonia and plasma-assisted molecular beam epitaxy